Uplink Capacity and Required Transmit Power of DS-CDMA DAN

Shohei INOSHITA† Hiroyuki MIYAZAKI† and Fumiyuki ADACHI‡
Dept. of Communications Engineering, Graduate School of Engineering, Tohoku University
6-6-05 Aza-Aoba, Aramaki, Aoba-ku, Sendai, 980-8579 Japan
†{inoshita, miyazaki}@mobile.ecei.tohoku.ac.jp, ‡adachi@ecei.tohoku.ac.jp

Abstract—**Antenna diversity is a powerful technique to mitigate the impact of multipath fading. In a conventional centralized antenna network (CAN), diversity antennas are co-located at base station and hence, the impacts of the propagation path loss and the shadowing loss cannot be mitigated. Distributed antenna network (DAN) is an effective way to mitigate all of the above impacts. The choice of the multi-access technique is a very important issue. In this paper, we consider broadband DS-CDMA with joint minimum mean square error based frequency domain-equalization (MMSE-FDE)/antenna diversity as the multi-access technique for DAN and investigate the link capacity and required transmit power to compare with CAN. It is shown by the computer simulation that DS-CDMA DAN can reduce the required transmit power for the given bit error rate (BER) and can obtain larger uplink cellular capacity than DS-CDMA CAN.**

Keywords-component; DS-CDMA, DAN, Uplink capacity, CCI, MUI, TPC, extended diversity

I. INTRODUCTION

In a conventional centralized antenna network (CAN), since diversity antennas are co-located at base station, the impact of fading can be mitigated by using antenna diversity; however, the impacts of the propagation path loss and the shadowing loss cannot be mitigated. Therefore, a high transmit power is required for a user near the cell edge to meet the required transmission quality, producing large co-channel interference (CCI) to other cells. One attractive solution is to introduce the distributed antenna network (DAN) [1-3]. In DAN, many antennas are spatially distributed in each cell. Some antennas near a user can be found with a high probability and hence, the propagation path loss and the shadowing loss can be mitigated. Thus, the transmit power can be significantly reduced, thereby reducing the CCI to other cells.

Since the available bandwidth is limited, the choice of multi-access (MA) technique is an important technical issue. Well known MAs are time division multiple access (TDMA), frequency division multiple access (FDMA), and code division multiple access (CDMA) [4]. In FDMA, the available channels are grouped into several channel groups which are allocated to different base stations. The same group needs to be reused at spatially separated base stations so as to minimize the CCI. Basically TDMA requires the similar channel allocation to FDMA. There are many channel allocation algorithms [5-7]. The fixed channel allocation is quite difficult to adapt to changing CCI environment unlike the dynamic channel allocation. However, the dynamic channel allocation is quite difficult to implement if not impossible and therefore, no practical dynamic channel allocation has been developed. On the other hand, thanks to the CCI reduction through dispreading process, CDMA can use the single frequency reuse (i.e., available bandwidth can be reused every cell) and hence, can avoid the sophisticated channel allocation. DS-CDMA is adopted for the third generation (3G) systems [4]. Coherent Rake combining combined with antenna diversity can mitigate the impact of multipath fading [8]. However, the severe multi-user interference (MUI) is produced due to the near-far problem caused by the path loss and the shadowing loss [9]. Therefore, the application of fast transmit power control (TPC) is essential [8-9]. Furthermore, CCI is the strongest for a user near the cell edge and therefore, the site diversity (or the soft handover) is also necessary [8].

In broadband DS-CDMA, the inter-chip interference (ICI) caused by the frequency-selective fading degrades the transmission performance. The minimum mean square error (MMSE) based frequency-domain equalization (FDE) can mitigate the ICI [10-11].

There have been many studies on DS-CDMA DAN [e.g., 12-15]. It was shown [12-14] that DS-CDMA DAN can achieve higher received signal-to-interference power ratio (SIR) than DS-CDMA CAN. Ref. [15] investigated the uplink power control for DS-CDMA DAN and showed that DAN can bring significant power saving. However, Refs. [12-15] consider the received SIR assuming Rake combining and do not evaluate the bit error rate (BER) performance. To the best of our knowledge, the uplink capacity of DS-CDMA DAN with joint MMSE-FDE/antenna diversity and comparison to DS-CDMA CAN have not been studied yet.

In this paper, we consider broadband DS-CDMA with joint MMSE-FDE/antenna diversity and investigate, by computer simulation, the uplink capacity of DS-CDMA DAN to show that DAN can achieve higher uplink capacity than CAN. We also show by the computer simulation that if antenna diversity is extended to involve multiple cells similar to site diversity, the link capacity can be further improved while reducing the transmit power.

The remainder of this paper is organized as follows. The uplink model of DS-CDMA DAN is described in Sect. II. Section III presents the DS-CDMA transmission system model. The computer simulation results on the BER outage probability, the transmit power distribution, and the uplink capacity is presented in Sect. IV. Sect. V offers some conclusions.

II. UPLINK DAN MODEL

A. Uplink Model

In this paper, multiuser and multi-cell environment is considered. Figure 1 illustrates the models of DAN and CAN with N_{total}=7 antennas in a multi-cell environment. The center cell (c=0) is assumed to be the cell of interest. Assuming the cluster size N=1, there are 6 CCI cells (c=1~6) for the cell of interest (c=0). In our DAN model, it is assumed that each distributed antenna covers the hexagonal area with a radius of $R' = R/\sqrt{7}$, where R represents the cell radius of the CAN. All distributed antennas are connected to the SPC by optical links (ideal signal transmission between each distributed antenna and the SPC is assumed). In CAN, all antennas are co-located at the center of the cell.

It is assumed that there are U active users in each cell and user terminal is equipped with single antenna (i.e., N_t=1). In this paper, distributed antennas are selected from D_{max}=7 surrounding cells including the cell of interest for diversity combining (we call this diversity as an extended diversity). Each user selects N_r antennas in order of decreasing the instantaneous received power from $D_{max}N_{total}$ antennas. Note that there are 6 CCI cells in the first tier of each surrounding cell (c=1~6) which has antennas user in the interest cell (c=0) communicates with. For example, if the user in c=0 cell selects an antenna in c=1 cell, there are 6 CCI cells (c=7, 8, 2, 0, 6, 18) for the antenna.

In this paper, we measure the distribution of local average BER by computer simulation to find the outage probability of BER, which is defined as the probability with which the local average BER exceed the required BER. We define the uplink capacity as the maximum number $U_{\max}$ of supportable users normalized by the spreading factor SF for the given allowable outage probability Q.

B. Channel Model

The broadband propagation channel is characterized by the propagation path loss, the log-normally distributed shadowing loss, and the frequency-selective fading. Assuming a frequency-selective channel composed of L distinct paths, the channel impulse response, $\tilde{h}^{\left(c,u \atop \to c',n_r\right)}(t)$, of the link between the u-th user in c-th cell and the n_r-th received antenna in c'-th cell is expressed as

$$\tilde{h}^{\left(c,u \atop \to c',n_r\right)}(t) = \sum_{l=0}^{L-1} \tilde{h}_l^{\left(c,u \atop \to c',n_r\right)} \cdot \delta\left(t - \tau_l^{\left(c,u \atop \to c',n_r\right)}\right), \tag{1}$$

where $\tilde{h}_l^{\left(c,u \atop \to c',n_r\right)}$ is the l-th complex valued path gain, including the impact of the propagation path loss and the shadowing loss, of the link between the u-th user in c-th cell and the n_r-th received antenna in c'-th cell. It is expressed as

$$\tilde{h}_l^{\left(c,u \atop \to c',n_r\right)} = \sqrt{D^{\left(c,u \atop \to c',n_r\right)^{-\alpha}} \cdot 10^{-\frac{\eta^{\left(c,u \atop \to c',n_r\right)}}{10}}} \cdot g_l^{\left(c,u \atop \to c',n_r\right)}, \tag{2}$$

where $D^{\left(c,u \atop \to c',n_r\right)}$ is the distance between the u-th user in c-th cell and the n_r-th received antenna in c'-th cell. α denotes the path loss exponent and $\eta^{\left(c,u \atop \to c',n_r\right)}$ is the shadowing loss in dB between the u-th user in c-th cell and the n_r-th received antenna in c'-th cell. $g_l^{\left(c,u \atop \to c',n_r\right)}$ and $\tau_l^{\left(c,u \atop \to c',n_r\right)}$ are the l-th complex-valued path gain with $E\left[\sum_{l=0}^{L-1}\left|g_l^{\left(c,u \atop \to c',n_r\right)}\right|^2\right] = 1$ and the time delay of the l-th path, respectively.

The instantaneous received signal power at the n_r-th received antenna in c'-th cell from the u-th user in c-th cell, $P_r^{\left(c,u \atop \to c',n_r\right)}$, is expressed as

$$\begin{aligned} P_r^{\left(c,u \atop \to c',n_r\right)} &= p_t^{(c,u)} \cdot \sum_{l=0}^{L-1}\left|\tilde{h}_l^{\left(c,u \atop \to c',n_r\right)}\right|^2 \\ &= p_t^{(c,u)} \cdot D^{\left(c,u \atop \to c',n_r\right)^{-\alpha}} \cdot 10^{-\frac{\eta^{\left(c,u \atop \to c',n_r\right)}}{10}} \cdot \sum_{l=0}^{L-1}\left|g_l^{\left(c,u \atop \to c',n_r\right)}\right|^2 \end{aligned}, \tag{3}$$

where $p_t^{(c,u)}$ represents the actual transmit power of the u-th user in c-th cell, and Eq. (3) can be rewritten as

$$\begin{aligned} & P_r^{\left(c,u \atop \to c',n_r\right)} \\ &= P_t^{(c,u)} \cdot d^{\left(c,u \atop \to c',n_r\right)^{-\alpha}} \cdot 10^{-\frac{\eta^{\left(c,u \atop \to c',n_r\right)}}{10}} \cdot \sum_{l=0}^{L-1}\left|g_l^{\left(c,u \atop \to c',n_r\right)}\right|^2 \\ &= P_t^{(c,u)} \cdot \sum_{l=0}^{L-1}\left|\hat{h}_l^{\left(c,u \atop \to c',n_r\right)}\right|^2 \end{aligned}, \tag{4}$$

where $P_t^{(c,u)} = p_t^{(c,u)} \cdot R^{-\alpha}$ and $d^{\left(c,u \atop \to c',n_r\right)} = D^{\left(c,u \atop \to c',n_r\right)}/R$, denote the normalized transmit power and the normalized distance, respectively. $\hat{h}_l^{\left(c,u \atop \to c',n_r\right)}$ is the normalized l-th complex valued path gain and expressed as

$$\hat{h}_l^{\left(c,u \atop \to c',n_r\right)} = \sqrt{\left(D^{\left(c,u \atop \to c',n_r\right)}\Big/R\right)^{-\alpha} \cdot 10^{-\frac{\eta^{\left(c,u \atop \to c',n_r\right)}}{10}}} \cdot g_l^{\left(c,u \atop \to c',n_r\right)}. \tag{5}$$

III. DS-CDMA WITH JOINT MMSE-FDE/ANTENNA DIVERSITY

A. Transmit/Receive Signal Representation

The DS-CDMA uplink transmitter/receiver structure is illustrated in Fig. 2. In the paper, the chip-spaced discrete-time signal representation is used.

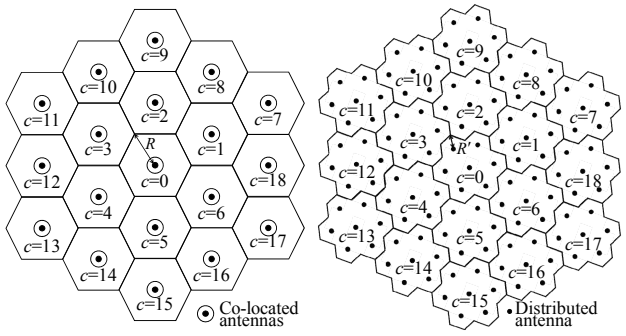

(a)CAN (b)DAN

Figure 1. Network models.

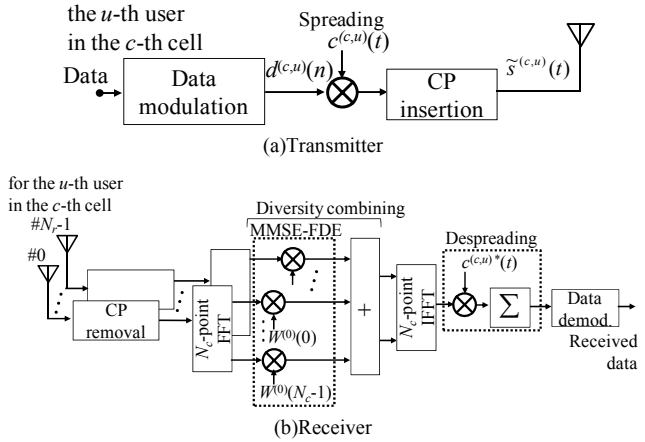

(a)Transmitter

(b)Receiver

Figure 2. Transmitter/receiver structure

All of the users in each cell are transmitting their signals. We consider the transmission of one block of N_c chips, where N_c denotes the block length for fast Fourier transform (FFT). At the transmitter of the u-th user (u=0~(U–1)) in c-th cell (c=0~18), a binary data sequence is transformed into data-modulated symbol sequence $\{d^{(c,u)}(n);\ n=0\sim(N_c/SF-1)\}$, and then spread by multiplying it with a user-specific long pseudo noise (PN) sequence $c^{(c,u)}(t)$. The resultant DS-CDMA signal, $\{\tilde{s}^{(c,u)}(t);\ t=0\sim(N_c-1)\}$, can be expressed using the equivalent baseband representation as

$$\tilde{s}^{(c,u)}(t)=\sqrt{2P_t^{(c,u)}}s^{(c,u)}(t), \tag{6}$$

where

$$s^{(c,u)}(t)=d^{(c,u)}(\lfloor t/SF\rfloor)c^{(c,u)}(t), \tag{7}$$

and $\lfloor x\rfloor$ represents the largest integer smaller than or equal to x. The last N_g chips of each block are copied as a cyclic prefix (CP) and inserted into the guard interval at the beginning of each block.

In the following, we assume that the u-th user in the c-th cell is the desired user 0. The n_r-th antenna which is selected by the desired user receives the signals from the desired user 0 and $u'(n_r)$ interference user ($u'(n_r)$=1~($7U$–1)) in the 7 surrounding cells where the n_r-th antenna exists.

The received signal at the n_r-th received antenna $\{r^{(n_r)}(t);\ t=0\sim(N_c-1)\}$ after CP removal can be expressed as

$$\begin{aligned} r^{(n_r)}(t) &= \sqrt{2P_t^{(0)}}\sum_{l=0}^{L-1}h_l^{(0,0\to n_r)}s^{(0)}\left(\left(t-\tau_l^{(0,0\to n_r)}\right)\bmod N_c\right) \\ &+\sum_{u'(n_r)=1}^{7U-1}\sqrt{2P_t^{(u'(n_r))}}\sum_{l=0}^{L-1}h_l^{(u'(n_r),0\to n_r)}s^{(u'(n_r))}\left(\left(t-\tau_l^{(u'(n_r),0\to n_r)}\right)\bmod N_c\right) \\ &+n^{(n_r)}(t) \end{aligned}, \tag{8}$$

where $s^{(0)}(t)$ and $s^{(u'(n_r))}(t)$ represent the transmit signals of the desired user 0 and interference user $u'(n_r)$, respectively. $P_t^{(v)}$ is the normalized transmit power of user v (v=0~($7U$–1)). $h_l^{(v',v\to n_r)}$ and $\tau_l^{(v',v\to n_r)}$ denote the normalized l-th complex valued path gain between the v'-th user and the n_r-th selected antenna and its time delay, respectively. $n^{(n_r)}(t)$ is the zero-mean complex-valued additive white Gaussian noise (AWGN) having variance $2N_0/T_c$ with N_0 and T_c representing the single-sided power spectrum density of the AWGN and the chip duration, respectively. After CP removal, the received signal is transformed into the frequency-domain signal by N_c-point FFT. The frequency-domain received signal $\{R^{(n_r)}(k);\ k=0\sim(N_c-1)\}$ can be expressed as

$$\begin{aligned} R^{(n_r)}(k) &= \sqrt{2P_t^{(0)}}H^{(u,0\to n_r)}(k)S^{(0)}(k) \\ &+\sum_{u'(n_r)=1}^{7U-1}\sqrt{2P_t^{(u'(n_r))}}H^{(u'(n_r),0\to n_r)}(k)S^{(u'(n_r))}(k) \\ &+\Pi^{(n_r)}(k) \end{aligned}, \tag{9}$$

where $S^{(v)}(k)$ is the kth frequency component of $s^{(v)}(t)$. $H^{(v,0\to n_r)}(k)$ and $\Pi^{(n_r)}(k)$ are respectively the k-th frequency channel transfer function and the noise component. They are given as

$$\begin{cases} S^{(v)}(k)=\sum_{t=0}^{N_c-1}s^{(v)}(t)\exp\left(-j2\pi k\dfrac{t}{N_c}\right) \\ H^{(v,0\to n_r)}(k)=\sum_{l=0}^{L-1}h_l^{(v,0\to n_r)}\exp\left(-j2\pi k\dfrac{\tau_l^{(v,0\to n_r)}}{N_c}\right) \\ \Pi^{(n_r)}(k)=\sum_{t=0}^{N_c-1}n^{(n_r)}(t)\exp\left(-j2\pi k\dfrac{t}{N_c}\right) \end{cases}. \tag{10}$$

Then, joint MMSE-FDE and diversity combining is performed to obtain a sequence of decision variables for data demodulation.

B. Joint MMSE-FDE/antenna diversity

Letting the equalization weight at the n_r-th antenna for the desired user 0 be $W^{(n_r)}(k)$, the frequency component $\hat{R}(k)$ after FDE and diversity combining is given as

$$\hat{R}(k)=\sum_{n_r=0}^{N_r-1}W^{(n_r)}(k)R^{(n_r)}(k). \tag{11}$$

The FDE weight $W^{(n_r)}(k)$ is determined so as to minimize the mean square error (MSE) between the desired transmit signal $\sqrt{2P_t^{(0)}}S^{(0)}(k)$ and the received signal $\hat{R}(k)$ after joint

FDE and diversity combining. The FDE weight $W^{(n_r)}(k)$ can be derived as [10]

$$W^{(n_r)}(k) = \frac{\Gamma^{(0)} H^{(0,0\to n_r)^*}(k)}{\left[\sum_{n_r=0}^{N_r-1} \Gamma^{(0)} \left| H^{(0,0\to n_r)}(k) \right|^2 + \sum_{n_r=0}^{N_r-1} \sum_{u'(n_r)=1}^{7U-1} \Gamma^{(u'(n_r))} \left| H^{(u'(n_r),0\to n_r)}(k) \right|^2 + 1 \right]}, \quad (12)$$

where

$$\Gamma^{(v)} = \frac{P_t^{(v)} T_c}{N_0}. \quad (13)$$

After joint FDE and diversity combining, the frequency-domain signal is transformed by N_c-point inverse FFT (IFFT) into the time-domain signal. Finally, the signal is despread, and demodulated.

C. SNR-based fast TPC

In this paper, we consider fast TPC so that the instantaneous signal-to-noise power ratio (SNR) after despreading is kept at the target SNR. The normalized transmit power $P_t^{(v)}$ of the v-th user is given by

$$P_t^{(v)} = \frac{N_0}{2T_c} \frac{SNR_{\text{target}}}{\sum_{n_r=0}^{N_r-1} \sum_{l=0}^{L-1} \left| h_l^{(v,v\to n_r)} \right|^2} \frac{1}{SF}. \quad (14)$$

IV. Computer Simulation

The simulation condition is summarized in Table 1. QPSK data modulation is considered. Long PN sequence is used as the spreading code and spreading factor SF is set to SF=16. FFT block size N_c and CP length N_g are respectively set to N_c=256 and N_g=32. The channel is assumed to be a frequency-selective fading having symbol spaced L=16 path uniform power delay profile. The path loss exponent α and the shadowing loss standard deviation σ are assumed to be α=3.5 and σ=7.0dB, respectively. We assume the interference-limited channel (SNR_{target}>>1) and ideal TPC. Perfect channel estimation is also assumed.

The outage probability is defined as the probability that the local average BER exceeds the required BER. The uplink capacity is defined as the maximum number $U_{\max}$ of supportable users normalized by the spreading factor SF. In this paper, the required BER and the allowable outage probability are set as BER=10^{-2} and Q=0.1, respectively.

Figure 3 illustrates the outage probability as a function of the normalized number of users U/SF, when N_r=3. For CAN, the outage probability significantly increases with U/SF. In contrast, DAN can achieve lower outage probability than CAN. The reason for this is given below. In CAN, antennas are co-located at the BS. On the other hand, in DAN, distributed antennas are geographically separated and hence, the interference from other users can be more mitigated by antenna diversity against not only the fading but also the propagation path loss and the shadowing loss.

Figure 4 plots the probability density function (PDF) of the normalized transmit power-to-TPC target ratio $P_t^{(v)}/P_{\text{target}}$ when N_r=3, where $P_{\text{target}} = SNR_{\text{target}}(N_0/2T_c)/SF$. It can be seen from Fig. 4 that DAN with extended diversity can reduce the required transmit power.

Figure 5 plots the uplink capacity, $U_{\max}/SF$, with the number of receive antennas N_r as parameter. It is shown in Fig. 5 that the uplink capacity of CAN without extended diversity is upper limited when N_r>3. In CAN without extended diversity, the user who is located cell edge requires large transmit power, and thereby, the transmit performance is degraded by large CCI. On the other hand, DAN can mitigate the impact of CCI, and hence can achieve 6 times higher uplink capacity than that of CAN without extended diversity.

It is also seen from Fig. 5 that the difference of uplink capacity between DAN with extended diversity and CAN with extended diversity decreases as N_r increases. The reason for this is explained as follows. In CAN, all antennas of each cell are co-located at the center of the cell, and hence, the received SIRs are the same among selected antennas. Therefore, the spatial diversity gain which is proportional with the number of selected antennas can be obtained. On the other hand, in DAN, antennas are spatially distributed in the cell. Therefore, the received SIRs are different among selected antennas and decreases as the distance between desire user and the selected antenna increases. As a consequence, the spatial diversity gain is upper limited by the interference from other users when N_r is large.

According to the above simulation results, it can be concluded that DAN achieve higher uplink capacity than CAN while using smaller number of received antennas.

V. Conclusions

In this paper, we investigated the uplink capacity of DS-CDMA DAN with joint MMSE-FDE/antenna diversity. In DAN, several antennas are found near a user with a high probability and hence, the negative impact of the path loss and the shadowing loss can be mitigated. We showed by the computer simulation that DAN can reduce the required transmit power and achieve a higher uplink capacity than CAN. Furthermore, the uplink capacity becomes higher as the number of received antennas increases due to antenna diversity while reducing the transmit power. However, when too many antennas are involved in diversity, some of the selected antennas may be far from a user and thereby, the spatial diversity gain may be saturated. As a result, the capacity difference between DAN and CAN decreases as N_r increases.

In DAN, the number of simultaneously accessing users per antenna is few and hence, the use of a simple interference cancellation technique can improve the uplink capacity. The interference cancellation for DS-CDMA DAN is left as our future study. In additon, we will also study the effect of signal-to-interference plus noise power ratio (SINR) based TPC.

TABLE I. COMPUTER SIMULATION CONDITION

Transmitter	Modulation	QPSK
	No. of FFT points	N_c=256 chips
	Guard interval length	N_g=32 chips
	Spreading factor	SF=16
	Spreading codes	Long PN code
	SNR-based fast TPC	SNR_{target}>>1
Channel	Fading type	Frequency-selective block Rayleigh
	Power delay profile	L=16-path uniform power delay profile
	Time delay	$\tau_l=l$ (l=0~L−1)
	Path-loss exponent	α=3.5
	Standard deviation of shadowing loss	σ=7.0 dB
Receiver	No. of distributed antennas	N_{total}=7
	Maximum no. of diversity cells	D_{max}=7
	Channel estimation	Ideal
	Joint MMSE-FDE/antenna diversity	
Required quality	Required BER	10^{-2}
	Allowable outage probability	Q=0.1

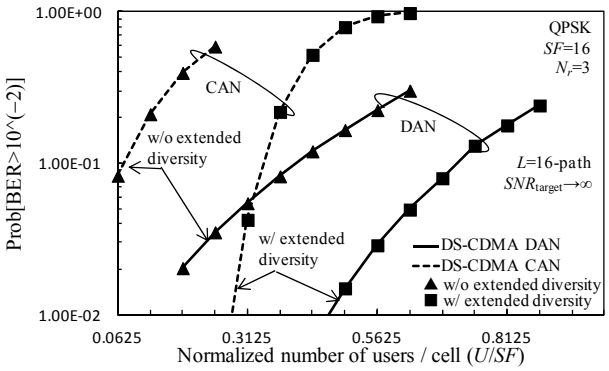

Figure 3. Outage probability.

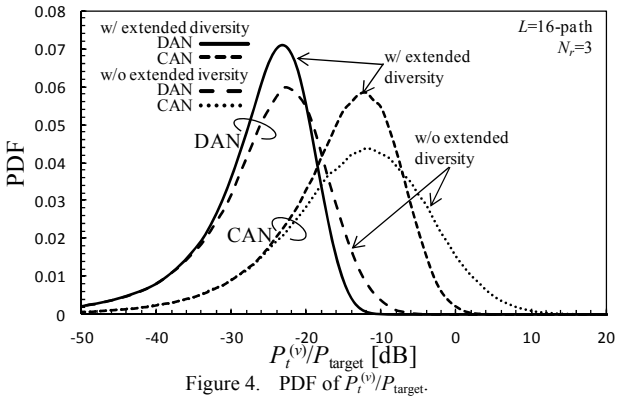

Figure 4. PDF of $P_t^{(v)}/P_{target}$.

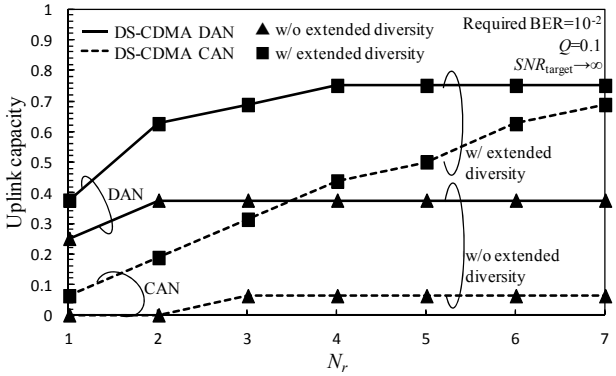

Figure 5. Uplink capacity.

REFERENCES

[1] W. Choi, "Downlink performance and capacity of distributed antenna systems in a multicell environment," IEEE Trans. Commun., Vol. 6, No. 1, pp. 69-73, January 2007.

[2] F. Adachi and K. Takeda, T. Yamamoto, R. Matsukawa, and S. Kumagai, "Recent advances in single-carrier distributed antenna network," Wireless Communications and Mobile Computing, Vol. 11, No. 12, pp. 1551-1563, December 2011.

[3] T. Yamamoto and F. Adachi, "Uplink Throughput Performance of Single-Carrier MIMO Spatial Multiplexing in Distributed Antenna Network," 9th IEEE Asia Pacific Wireless Communication Symposium (APWCS 2012), Kyoto, Japan, August 2012.

[4] F. Adachi, "Wireless past and future - evolving mobile communications systems," IEICE Trans. Fundamentals, Vol. E84-A, pp. 55-60, January 2001.

[5] Y. Matsumura, S. Kumagai, T. Obara, T. Yamamoto, and F. Adachi, "Channel Segregation Based Dynbamic Channel Assignment for WLAN," 2012 IEEE The 13th International Conference on Communication Systems, Sigapore, 21-23 November 2012.

[6] R. Matsukawa, S. Kumagai, T. Obara, T.Yamamoto, and F. Adachi, "A dynamic channel assignment scheme for distributed antenna networks," Proc. IEEE 75th Cehicular Technology Confrerence, May 2012.

[7] Y. Furuya and Y. Akaiwa, "Channel segregation, a distributed adaptive channel assignment scheme for mobile communication systems," IEIEC Trans. Communications, Vol. E74-B, No. 6, pp. 1531-1537, June 1991.

[8] F. Adachi, M. Sawahashi and H. Suda, "Wideband DS-CDMA for next-generation mobile communications systems," IEEE Commun. Mag., Vol. 36, pp. 56-69, September 1998.

[9] A. Goldsmith, *Wireless Communication*, Cambridge University Press, 2005.

[10] F. Adachi and K. Takeda, "Bit error rate analysis of DS-CDMA with joint frequency-domain equalization and antenna diversity combining," IEICE Trans. Commun., Vol. E87-B, No. 10, pp. 2991-3002, October 2004.

[11] K. Takeda and F. Adachi, "Performance evaluation of multi-rate DS-CDMA using frequency-domain equalization in a frequency-selective fading channel," IEICE Trans. Commun., Vol. E88-B, No. 3, pp. 1191-1201, March 2005.

[12] L. Dai, S. Zho, and Y. Yao, "Capacity analysis in CDMA distributed antenna system," IEEE Trans. Wireless Commun., Vol. 4, No. 6, pp. 2613-2620, November 2006.

[13] G. H. Chen, C.-M. Yu, and C.-C. Huang. "A simulation study of a distributed antenna-based CDMA system," in Proc. IEEE Symp. Pers., Indoor Mobile Radio Commun., Vol. 2, pp. 517-521, October 1996.

[14] R. Hasegawa, M. Shirakabe, R. Esmailzadeh, and M. Nakagawa, "Downlink performance of a CDMA system with distributed base station," in Proc. IEEE Vech. Technol. Conf., Vol. 2, pp. 882-886, October 2003.

[15] A. Obaid and H. Yanikomeroglu, "Reverse-link power control in CDMA distributed antenna systems," in Proc. IEEE Wireless Commun. Networking Conf., Vol. 2, pp. 608-612, September 2000.